J. Membrane Biol. 148, 233–242 (1995)

The Journal of
Membrane
Biology

The Paracellular Channel for Water Secretion in the Upper Segment of the Malpighian Tubule of *Rhodnius prolixus*

C. Sofía Hernández[1], E. González[2], G. Whittembury[1]
[1]Instituto Venezolano de Investigaciones Científicas, IVIC, Caracas 1020-A Venezuela
[2]Escuela de Medicina J.M. Vargas, UCV, Caracas, Venezuela

Received: 17 May 1995 / Revised: 26 July 1995

Abstract. Lumen to bath J_{12}/C_1 and bath to lumen J_{21}/C_2 fluxes per unit concentration of 19 probes with diameters (d^m) ranging from 3.0–30.0 Å (water, urea, erythritol, mannitol, sucrose, raffinose and 13 dextrans with d^m 9.1–30.0 Å) were measured during volume secretion (J_v) in the upper segment of the Malpighian Tubule of *Rhodnius* by perfusing lumen and bath with ^{14}C or ^3H-labeled probes. $J_{net} = (J_{12}/C_1 - J_{21}/C_2)$ was studied as a function of $J_v \cdot J_v$ was varied by using different concentrations of 5-hydroxy tryptamine. J_{net} for ^3H-water was not different from J_v. We found: (i) A strong correlation between J_{net} and J_v for 8 probes d^m = 3.0–11.8 Å (*group a* probes), indicating that the convective component of J_{net} is more important than its diffusive component and than unstirred layers effects which are negligible. Therefore *group a* probes are solvent dragged as they cross the epithelium. (ii) There is no correlation between J_{net} and J_v for 11 probes with d^m = 11.8–30 Å (*group b*). Therefore these probes must cross the epithelium by diffusion and not by solvent drag. (iii) In a plot of J_{net}/J_v *vs.* d^m *group a* probes show a steep linear relation with a slope = –0.111, while for *group b* probes the slope is –0.002. Thus there is a break between *groups a* and *b* in this plot. We tried to fit the data with models for restricted diffusion and convention through cylindrical or parallel slit pathways. We conclude that (i) *group a* probes are dragged by water through an 11.0 Å-wide slit. (ii) Most of J_v must follow an extracellular noncytosolic pathway. (iii) *Group b* probes must diffuse through a 42 Å-wide slit. (iv) A cylindrical pathway does not fit the data.

Key words: Paracellular flow — Malpighian tubules — Secretion — Epithelial transport — Water transport — Convective flow

Correspondence to: G. Whittembury

Introduction

The UMT of *Rhodnius* secretes a quasi-isosmotic fluid, at rates as high as 50 nl/cm^2 · sec after stimulation by 5-hydroxy-tryptamine (5-HT) and other hormones (Maddrell, 1980; Maddrell et al., 1991, 1993) through routes still under debate. On the one hand, O'Donnell, Aldis & Maddrell (1982), O'Donnell & Maddrell (1983) and O'Donnell, Maddrell & Gardiner (1984) propose that secretion is mainly transcellular, based in transepithelial water osmotic permeability measurements and in the possible effect of unstirred layer (USL) effects in the unilateral upper segment of the Malpighian Tubule (UMT) preparation. On the other hand, Whittembury et al., (1986) propose that water follows a paracellular pathway in the UMT unilateral preparation, based in the observation that the convective component of the transepithelial net flow per unit concentration, J_{net}, of six non-electrolyte probes (urea, erythritol, mannitol, glucose, sucrose and polyethylene glycol (PEG-800), is significantly larger than its diffusive component, under conditions in which unstirred layer (USL) effects (*pseudo-solvent drag,* Barry & Diamond, 1984) are negligible. These authors conclude that the 6 probes are dragged by water. In their view, solvent drag had to be paracellular, since the *true extracellular markers* sucrose and PEG-800 were among the dragged solutes. They further observed that J_{net} of raffinose (molecular diameter, d^m, 11.8 Å), inulin and dextran (15–18 kD), showed no convective component leading, to the estimation that the pathway where solvent drags the 6 solutes mentioned above was a 12 Å-wide slit (Whittembury et al., 1986).

In an effort to ascertain which of these opposing views holds, we restudied this matter using the following approach. (i) Unidirectional lumen to bath fluxes and bath to lumen fluxes were measured in a perfused lumen and bath preparation (instead of in the unilateral UMT

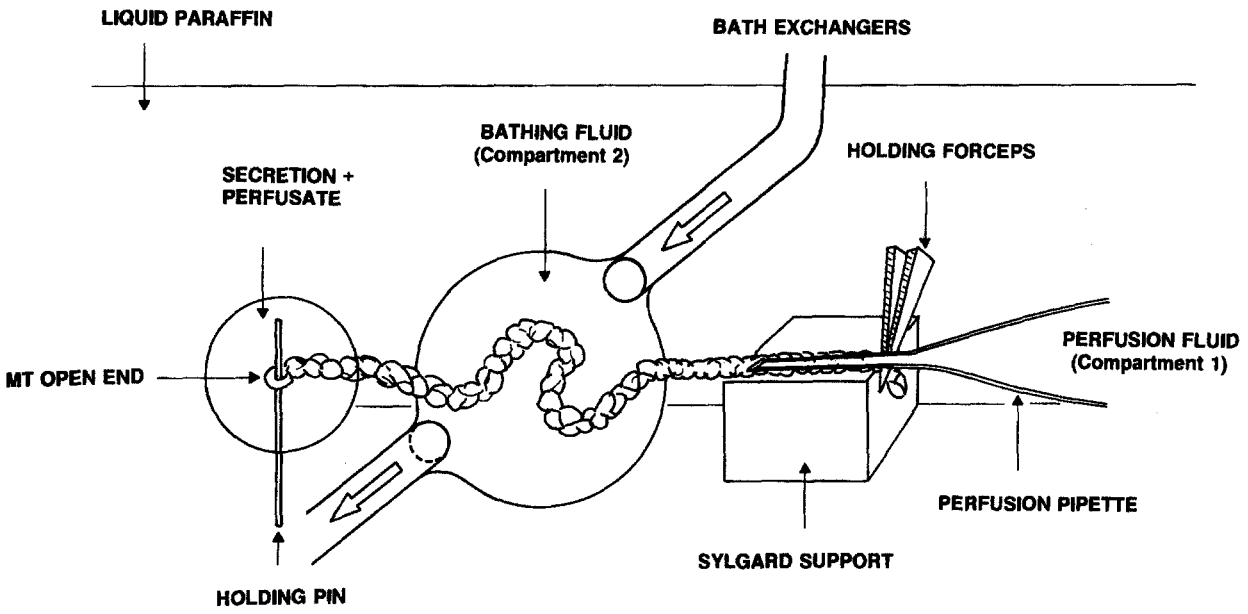

Fig. 1. Experimental setup (schematic). The UMT is held with forceps on top of a sylgard support. Its lumen is cannulated from its blind end by means of a micropipette under liquid paraffin. Fluid (Compartment 1) is perfused through the lumen by means of a Hampel pump. The bath (Compartment 2) can be exchanged. The little drops of secretion + perfusate are collected for analysis at the hydrophilic holding pin from the UMT open end.

preparation) to measure J_{net} from the difference between the unidirectional fluxes. Thus USL effects were ruled out. (ii) The range in d^m and the number of probes used to measure J_{net} was increased to 19 probes. (iii) Water was included among the probes. (iv) By using a technique developed by Shachar-Hill & Hill (1993) transepithelial fluxes of 13 dextrans, with molecular diameters ranging from 9.1 to 30.0 Å could be measured in a single experiment. (v) These measurements allowed to fit equations of various models for convective and diffusive flows through either cylindrical channels or parallel walled slits. (vi) These equations are independent of parameters that had to be estimated in the previous study (like the reflection coefficient σ) (Whittembury et al., 1986).

It is concluded that probes ranging from water to dextran 3 with a d^m between 3.0 and 11.8 Å are solvent-dragged through an 11.0 Å-wide slit, and not through a cylindrical pore. Diffusion is insignificant. Therefore secretion is mainly paracellular, as it requires such a wide pathway. Probes with a d^m between 11.8 and 30.0 Å are not solvent-dragged. They diffuse across the epithelial wall through a 42 Å-wide slit.

Materials and Methods

Fifth instar *Rhodnius prolixus* were used 1–4 weeks after moulting. They were cultured in the laboratory (Whittembury et al., 1986). UMT were isolated in oxygenated insect Ringer solution, IRS, (Maddrell, 1980). A tubule was then transferred to a chamber (Fig. 1), thermostated at 30°C. The blind end of the tubule was held with specially designed forceps, on top of a Sylgard support, under water saturated and oxygenated liquid paraffin. The tubule wall was cannulated with a sharp beveled perfusion pipette containing IRS (Compartment 1). The IRS was perfused through the lumen by means of a Hampel pump (Deetjen, 1978), and was collected periodically with the added tubule secretion at the tubule's open end (Fig. 1). Techniques for handling small volumes were used (Shipp et al., 1985). A region of the external surface of the tubule's length was bathed also with IRS (Compartment 2) which could be exchanged at a fixed rate, by means of micropipettes aligned perpendicular to the tubule's length (O'Donnell and Maddrell, 1983). Thus there was appropriate mixing of the external bathing solution as well as of the lumen to render USL effects negligible.

At time = 0, secretion was started by addition to compartment 2 of 5-HT to a concentration ranging from 10^{-5} to 10^{-7} mol/l to vary the secretory rate. The Insect Ringer Solution (IRS) had the following composition (Maddrell, 1980) in mmol/l: NaCl, 129; KCl, 8.6; NaH_2PO_4, 4.3; $NaHCO_3$, 10.2; $CaCl_2$, 2.0; glucose, 34; alanine, 3; pH, 7.35–7.45; osmolality, 340 mOsm/kg (freezing point determination). Chemicals (except for the dextrans) were from Merck and Sigma Chemical. The following radioactive substances (New England Nuclear) were used in 1 mole/l carrier (which virtually did not contribute to the osmolality); [^{3}H]water, [^{14}C]urea, [^{14}C]erythritol, [^{14}C]mannitol, [^{14}C]sucrose, and [^{3}H]raffinose. Shachar-Hill & Hill (1993) describe in detail the [^{3}H]dextrans and the analytical techniques. Briefly, Dextran T10 (Pharmacia LKB, Uppsala) was tritiated by Amersham International (Aylesbury, Bucks). The material contained all oligomers down to the monomer (glucose). The stock solution the freeze-dried to remove tritiated water and stored in the cold. As with the other labeled probes, the polydisperse [^{3}H]T10 dextrans used were dissolved either in the lumen (Compartment 1) or the external solution (Compartment 2) according to the experimental design (*see below*). The secretory flow, (J_v in nl/cm^2 · sec) was calculated from the total volume appearing at the open end of the tubule (minus the perfusion volume) the collection period and the area of tubular surface exposed to the bath. The tubule area was obtained from *camera lucida* tracing to measure

tubular length. It was assumed that the tubules were well represented by a cylinder. Tubule diameters were measured with an image splitter (Carpi-Medina et al., 1984). The volume of each collection was directly pipetted into 1 ml of distilled water and counted with 3 ml of counting solution in a Beckman LS 5000TD liquid scintillation counter. Known volumes of compartment 2 were similarly counted.

To measure lumen (Compartment 1) to bath (Compartment 2) fluxes per unit lumen concentration, (J^s_{12}/C_1), the tubule lumen was perfused at 120 nl/min with a labeled solution at an activity, C_1, and the bath was sampled at 15-min intervals and counted. To measure the bath-to-lumen fluxes per unit bath concentration, (J^s_{21}/C_2), the bath was labeled at an activity C_2 in parallel experiments. The lumen was perfused at 120 nl/min. Lumen samples were collected at 15-min intervals and counted. Net probe flux, $J_{net} = (J^s_{21}/C_2 - J^s_{12}/C_1)$, in units of 10^{-6}cm^3/cm^2 · sec, was taken as positive in the secretory direction. The experiments using labeled water, urea, erythritol, mannitol, sucrose and raffinose were analyzed directly. The dextran experiments required their fractionation. This is only summarized here as it is described in detail by Shachar-Hill & Hill (1993).

Fractionation of the Transported Dextrans

A sample from compartment 1 and compartment 2, diluted to a total volume of 100 µl was assayed by gel chromatography on Sephadex G25, with a fractionation range for dextrans of 0.1–5 kDa. The temperature was 20°C. The total gel volume (V_t) was 82 ml. Blue dextran (MW 2000 kDa) was routinely included to estimate the void volume, (V_o). The total elution volume was 110 ml of which that after the first 41 ml was collected in 0.92 ml fractions. They were counted by liquid scintillation as described above. A computer routine found the accessible volume coefficient, (K_{av}) for each fraction whose elution volume was V_x. This is given by $K_{av} = (V_x - V_o)/(V_t - V_o)$. As K_{av} values vary between runs because void and fraction volume vary slightly, the computer routine interpolated activity values at 0.01 K_{av} steps over the range after which different eluate curves could be aligned and activity ratios calculated as a function of K_{av}. K_{av} values were converted to dextran radii (or diameters, d^m) by use of the appropriate Ogston equation for Sephadex G25 (Equation A2, Shachar-Hill & Hill, 1993). Thus in our experimental conditions transtubule fluxes for 13 individual dextrans of 13 known d^m (ranging from 9.1 to 30.0 Å) could be defined in a single experiment. These different dextrans are denoted in the following sections with numbers *1* to *13*. Fluxes of dextrans with $d^m > 30.0$ Å were nondetectable.

USL Effects

As has been described above both compartments were renewed periodically at a sufficient rate to render USL effects negligible. In a thorough analysis of USL effects, O'Donnell, Aldis & Maddrell (1982) reached a similar conclusion for a similar experimental configuration, that however used transepithelial osmotic differences.

Symbols

(Equation numbers are in parentheses. Cylinder and slit denote a cylindrical and a parallel walled slit channel, respectively).

$(_1)$	subscript $_1$, lumen compartment
$(_2)$	subscript $_2$, bath compartment
A	pathway cross-sectional area
α	molecular diameter/cylinder diameter ratio = d^m/d (1, 3)
β	paracellular fraction of J_v
C(X)	probe concentration (along the channel)
C_c, C_t	C at cis- and trans- end of channel segment (5a, 5b)
C_1, C_2	probe concentration at lumen and bath perfusates
ΔC	transepithelial concentration difference
C*	average probe concentration in the epithelium
$(^c)$	superscript ^{c}, cylinder
D	probe free solution diffusion coefficient
d	cylinder diameter
d^m	molecular diameter
$(_d)$	subscript $_d$, diffusion
F^c,	restricted diffusive flow drag factor, cylinder (1, 5a)
F^s	restricted diffusive flow drag factor, slit (2, 5b)
$(_f)$	subscript $_f$, convection
ϕ^c	argument in exponential, cylinder (5a)
ϕ^s	argument in exponential, slit (5b)
G^c	convective flow drag factors, cylinder (3, 5a)
G^s	convective flow drag factors, slit (4, 5b)
J_{21}/C_2	bath→lumen probe flow per unit bath concentration
J_{12}/C_1	lumen→bath probe flow per unit lumen concentration
J_{net}	net probe flow per unit concentration = $(J_{21}/C_2 - J_{12}/C_1$
$J_{net}{}^c$	net probe flow, cylinder (5a, 6a, 6a1)
$J_{net}{}^s$	net probe flow, slit (5b, 6b, 6b1)
J_v	volume flow
j(x)	restricted movement by diffusion and convection
L	linear slit extent per cm^2 of area in a plane parallel to the membrane surface
λ	molecular diameter to slit width ratio = d^m/w (2, 4)
N	number of cylinders per cm^2 of epithelium (6a)
$N\pi d^2/4$	area of cylinders per cm^2 of epithelium (6a)
P	Permeability coefficient (6)
P^c	Permeability coefficient, cylinder (6a)
P^s	Permeability coefficient, slit (6b)
S^c_d	diffusive flow steric factors, cylinder (1, 5a)
S^s_d	diffusive flow steric factors, slit (2, 5b)
S^c_f	convective flow steric factors, cylinder (3, 5a)
S^s_f	convective flow steric factors, slit (4, 5b)
$S^c_d \cdot F^c$	hindrance to diffusion, cylinder (1, 5a)
$S^s_d \cdot F^s$	hindrance to diffusion, slit (2, 5b)
$S^c_f \cdot G^c$	hindrance to convection, cylinder (3, 5a)
$S^s_f \cdot G^s$	hindrance to convection, slit (4, 5b)
$(^s)$	superscript ^{s}, slit
σ	Reflection coefficient (6)
σ^c	Reflection coefficient, cylinder (6a)
σ^s	Reflection coefficient, slit (6b)
v(x)	fluid velocity
w	slit width
wL	surface area of slit per cm^2 of epithelium
X	cylinder or slit length
x	distance along the channel

Results

J_v varied from values near 0 to 48 nl/cm^2 · sec according to the different concentrations of 5-HT used (O'Donnell & Maddrell, 1983; Whittembury et al., 1986). Unidirectional fluxes of water, urea, erythritol, mannitol, sucrose, raffinose and 13 dextrans could be measured. Of the 19 probes explored, J^s_{12}/C_1 values of only water, urea, erythritol, mannitol and sucrose were significantly larger than 0. There was no relation between (J^s_{12}/C_1) and J_v. Average results are given in Table 1. J^s_{12}/C_1 of probes with $d^m > 9$ Å were nondetectable (*data not shown*). All values of J^s_{21}/C_2 for each of 19 probes, measured in parallel

Table 1. Lumen to bath fluxes per unit lumen concentration, J^s_{12}/C_1

SOLUTE	J^s_{12}/C_1 (10^{-6} cm/sec)	N
THO	33.61 ± 4.24	17
Urea	2.47 ± 0.13	19
Erythritol	0.84 ± 0.07	21
Mannitol	0.32 ± 0.08	10
Sucrose	0.26 ± 0.08	16

The tubule lumen (Compartment 1) was perfused at 120 nl/min with an isotope-containing solution. The bath (Compartment 2) was sampled at 30-min intervals. Fluxes of solutes with larger d^m were not statistically different from 0. They are not reported here. *N*, number of experiments.

experiments, were significantly larger than 0. J^s_{21}/C_2 for dextrans with $d^m > 30.0$ Å were not significantly different from 0 (*data not shown*). J^s_{21}/C_2 for water, urea, erythritol, mannitol, sucrose, and dextrans 1, 2 and 3 (d^m of 9.1, 9.9 and 11.8 Å, respectively) correlated significantly with J_v (*data not shown*). J^s_{21}/C_2 for raffinose and dextrans 4–13 did not correlate with J_v.

J_{net} for each probe was obtained by subtracting J^s_{12}/C_1 values at each J_v from the corresponding J^s_{21}/C_2 figures at the same J_v. In the case of water, J_{net} varied as a function of J_v with a highly significant correlation (*Table 2*). The slope $m = 0.884 \pm 0.290$, is statistically not different from 1.00. Therefore J_{net} for water equaled J_v within experimental error, confirming the precision of our methods. The mean water J_{net} was 25.1 ± 3.98 nl/cm^2 · sec. It corresponds to a J_{net}/J_v ratio of 0.932 ± 0.148 (Fig. 3) a value not statistically different from 1.0, which is equivalent for a J_v of 27 nl/cm^2 · sec.

There was also a highly significant correlation between J_{net} and J_v for urea, erythrytol, mannitol, sucrose, and dextrans *1*, *2*, and *3*, in addition to that just mentioned for water. These results are very similar to previously published ones for urea, erythritol, mannitol and sucrose in the unilateral UMT preparation (Whittembury et al., 1986). Table 2 gives the slopes and correlation coefficients of J_{net} with J_v for all 8 probes. The slope for urea (1.158 ± 0.136) is also not different from 1.00. The slopes decrease as d^m increases. They are erythrytol, 0.185 ± 0.036; mannitol, 0.149 ± 0.30; sucrose, 0.035 ± 0.004; and Dextrans *1*, 0.088 ± 0.032; *2*, 0.095 ± 0.030; and *3*, 0.022 ± 0.005. These 8 probes are called *group a* probes as their slopes are all significantly different from 0.

Table 3 gives the slopes for the 11 other probes, called *group b* probes as their slopes and correlation coefficients are not different from 0. It includes raffinose (d^m = 11.8 Å), and the Dextrans *4* to *13* (with d^m ranging from 13.0 to 30 Å).

Figure 2 shows a plot of J_{net} values divided by J_v, (J_{net}/J_v) as a function of d^m. It may be noticed that beginning at the origin, first (J_{net}/J_v) decreases sharply with d^m and then the values of (J_{net}/J_v) as a function of d^m

Table 2. Group *a* probes. Regression of J_{net} as a function of J_v

Probing molecule		Diameter Å	m	r	P	N
Water	(W)	3.0	0.884 ± 0.290	0.54	= 0.025	15
Urea	(U)	4.6	1.158 ± 0.136	0.85	< 0.001	29
Erythritol	(E)	6.4	0.185 ± 0.036	0.66	< 0.001	35
Mannitol	(M)	8.0	0.149 ± 0.030	0.79	< 0.001	16
Sucrose	(S)	9.0	0.037 ± 0.004	0.83	< 0.001	38
Dextran 1	(1)	9.1	0.088 ± 0.032	0.75	= 0.025	8
Dextran 2	(2)	9.9	0.095 ± 0.030	0.60	= 0.025	8
Dextran 3	(3)	11.8	0.022 ± 0.005	0.64	< 0.001	15

The equation is $J_{net} = (J_{21}/C_2 - J_{12}/C_1) = mJ_v + b$; r is the linear regression coefficient; P, the probability that $m = 0$; N, the number of experiments. In parentheses is the probe notation used in the figures.

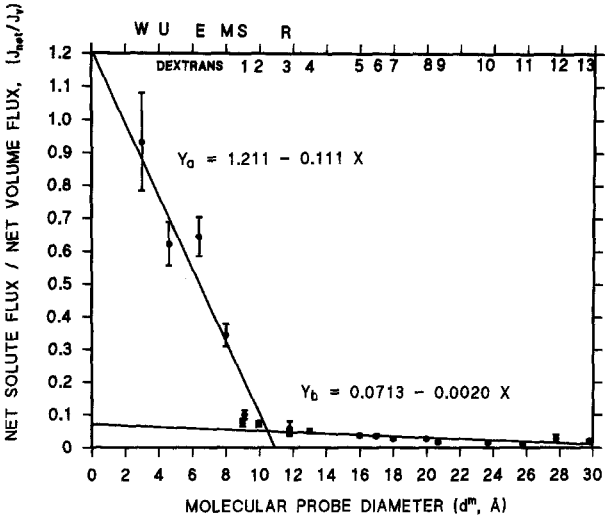

Fig. 2. Net solute to net volume flux ratio (J_{net}/J_v) (mean ± SEM) for 19 probes plotted as a function of their molecular diameter (d^m in Å). The abscissa at the top labels respectively the molecular diameter (d^m) of the probes water, urea, erythritol, mannitol, sucrose, raffinose and dextrans 1 to 13 as W, U, E, M, S, R, and 1, 2, ... 13. Two straight regression lines are shown: (*a*) The steep one (Y_a = 1.211 − 0.111*X*) best fits all eight *group a* probes (*see* Table 2). The less steep line (Y_b = 0.0713 − 0.0020*X*) best fits *group b* probes (*see* Table 3). $J_{net} = 0$ for dextrans with $d^m > 30$ Å. The ordinate $J_{net}/J_v = 1.0$ corresponds to the average J_v of 27 nl/cm^2 · sec.

taper down showing a much smaller slope. There is a break at d^m of about 12 Å. The straight line regression of J_{net}/J_v *vs.* d^m for all *group a* probes is Y_a = 1.211 (±0.139) − 0.111 (±0.014) *X*. The X-intercept is 10.9 Å, in good agreement with the observed break point. The *Y* intercept is not statistically different from 1.00. The value of r (−0.948 ± 0.120) is highly significant ($P < 0.001$). This part of Fig. 2 is shown with an expanded abscissa in Fig. 4.

A second straight line has been drawn for the second part of Fig. 2 using values of the 11 probes of *group b*.

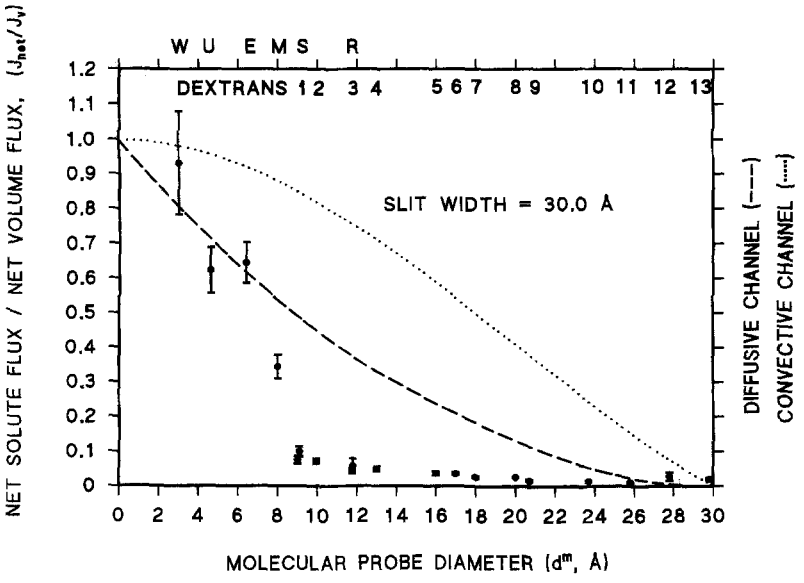

Fig. 3. Plot of (J_{net}/J_v) as a function of d^m for the 19 probes, as in Fig. 2. Neither the dotted nor the dashed line (convection and diffusion through a 30.0 Å-wide slit, occupying 100% of the flow areas, respectively) fit the data. To calculate these lines, Eqs. 2, 4 and 5*b* were used.

Table 3. Group *b* probes. Regression of J_{net} as a function of J_v

Probing molecule		Diameter Å	*m*	*r*	*N*
Raffinose	(R)	11.8	0.050 ± 0.037	0.23	34
Dextran 4	(4)	13.0	0.022 ± 0.035	0.26	8
Dextran 5	(5)	16.0	0.025 ± 0.015	0.46	8
Dextran 6	(6)	17.0	0.038 ± 0.024	0.41	8
Dextran 7	(7)	18.0	0.043 ± 0.022	0.43	8
Dextran 8	(8)	20.0	0.063 ± 0.034	0.36	8
Dextran 9	(9)	21.6	0.008 ± 0.006	0.35	8
Dextran 10	(10)	23.7	0.004 ± 0.010	0.17	8
Dextran 11	(11)	25.8	−0.002 ± 0.001	−0.13	8
Dextran 12	(12)	27.8	0.003 ± 0.002	0.20	8
Dextran 13	(13)	30.0	0.004 ± 0.003	0.15	8

(*See* Table 2). Neither *m* nor *r* were significantly different from 0.

The equation is $Y_b = 0.0713\ (\pm 0.0101) - 0.0020\ (\pm 0.0004)\ X$; $(r = -0.833 \pm 0.175)$. Although the slope is small, it is highly significant ($P < 0.001$). The X-intercept ($J_{net}/J_v = 0$) is 34.9 Å in good agreement with the observed absence of transepithelial flow of Dextrans with $d^m > 30$ Å. This second part of the graph is shown with an expanded ordinate in Figs. 5 and 6.

To sum up, our results show on the one hand, that the 8 probes of *group a* show a significant positive correlation between J_{net} and J_v. In addition, J_{net}/J_v drops sharply as a function of d^m (Fig. 2). On the other hand, the 11 probes of *group b* show no correlation between J_{net} and J_v. In addition J_{net}/J_v drops very gently with d^m. There is a break point between the two groups of probes. Dextran *3* ($d^m = 11.8$ Å) is the largest member of *group a*, while raffinose (also with $d^m = 11.8$ Å) is the smallest of *group b*.

Discussion

Our main findings are: (i) Water $J_{net} = J_v$ within experimental error. This underscores the precision of our experimental method. (ii) The 19 probes that cross the epithelium may be divided into two groups, namely *group a* (8 probes, with d^m from 3.0 to 11.8 Å) and *group b* (11 probes, with d^m from 11.8 to 30.0 Å). There is a strong positive significant relation between J_{net} and J_v for *group a* probes (Table 2). The slopes are larger than 0. It is known that J_{net} has a diffusive and a convective component (first and second term on the right hand side of Eq. 6). The values of these slopes indicate either that solvent drags these probes or that USLs mimic convection (*pseudo solvent drag*, Barry & Diamond, 1984). In the present experiments both compartments were well stirred (Materials and Methods). Thus *pseudo solvent drag* can be ruled out. Therefore, solvent drag of *group a* probes (including *extracellular markers* as large as sucrose and dextrans *1*, *2* and *3*) is the only source of the significant slopes relating J_{net} and J_v. Previous results with urea, erythritol, mannitol, glucose, PEG-800 and sucrose in the unilateral UMT preparation had led to a similar conclusion (Whittembury et al., 1986). (iii) There is no correlation between J_{net} and J_v for *group b* probes. The slopes are not different from 0 (Table 3). Therefore, on these grounds it may be concluded that these probes are not dragged by solvent. Previous observations in the unilateral UMT preparation with raffinose, inulin and dextran (d^m 28–30 Å) had led to a similar conclusion (Whittembury et al., 1986). (iii) A graph of J_{net}/J_v against d^m (Fig. 2) shows two parts: There is a steep negative linear relation between J_{net}/J_v and d^m for *group a* probes. There is also a negative correlation between J_{net}/J_v and d^m for *group b* probes but the slope is 1/50th of the first one. Thus, in Fig. 2 *group a* probes (those that are solvent-

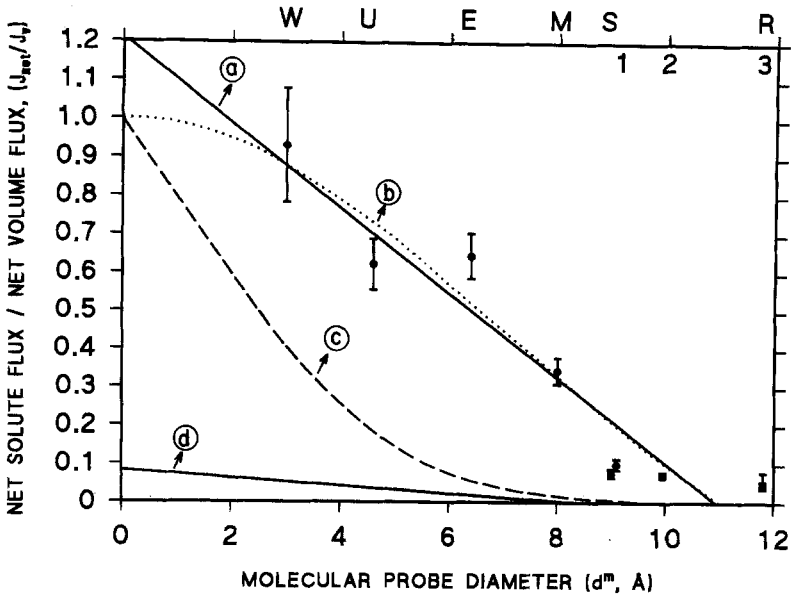

Fig. 4. Plot of (J_{net}/J_v) as a function of d^m, for *group a* probes. The abscissa is expanded (*see* Fig. 2). Line (*a*) is $Y_a = 1.211 - 0.111X$ of Fig. 2. Dotted line (*b*) is convection through an 11.0 Å-wide slit (calculated using Eqs. 4 and 5*b*). Both curves fit well the experimental data. Dashed line (*c*) is convection through a cylinder with a d^m = 11.0 Å (calculated using Eqs. 3 and 5*a*) and line (*d*) is diffusion through an 11.0 Å-wide slit (calculated using Eqs. 2 and 5*b*). Neither (*c*) nor (*d*) fit the data (*see* text).

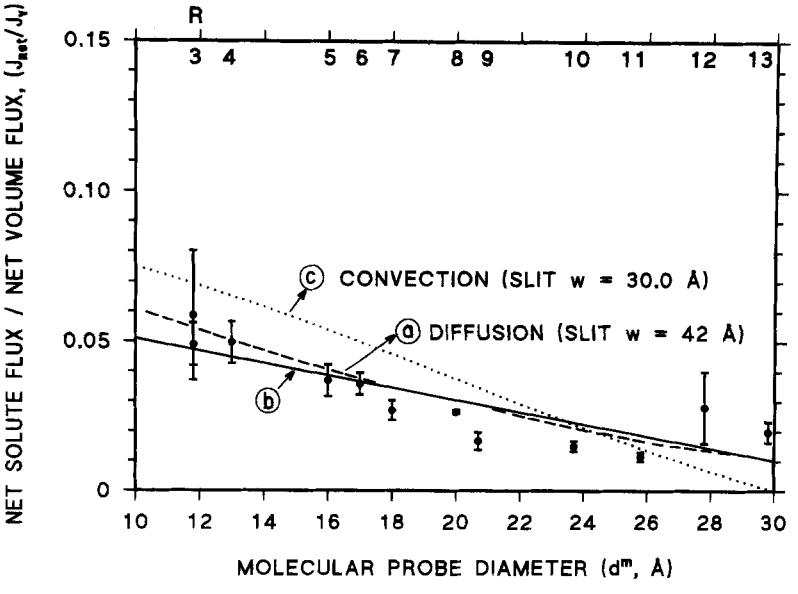

Fig. 5. Plot of (J_{net}/J_v) as a function of d^m for *group b* probes (d^m 11.8–30.0 Å). The abscissa is expanded (*see* Fig. 2). Broken line (*a*) is diffusion through a 42 Å-wide slit for 0.089 of the total flow area (calculated using Eqs. 2 and 5*b*). It fits well the experimental values. Line (*b*) is $Y_b = 0.0713 - 0.0020X$ of Fig. 2. Dotted line (*c*) is convection through a 30.0 Å-wide slit for the same fractional area as in (*a*) (calculated using Eqs. 4 and 5*b*). It is not a good fit to the data.

dragged) show a different behavior than *group b* probes (those that are not solvent-dragged).

Steric and Drag Factors in Diffusive and Convective Flow Models

We now analyze the findings described above in terms of models of cylindrical channels (denoted here simply as *cylinders*) and of parallel walled slits (denoted here as *slits*) that hinder the flow of particles that move through them by diffusion and convection. The models consider relative dimensions of probe and channel; probe position as it enters and flows along the channel; and channel velocity profile (Steward, 1982; Shachar-Hill & Hill, 1983). Hindrances to diffusion (Eqs. 1 and 2) and to convection (Eqs. 3 and 4) are ascribed to *steric* and *drag factors* thought to occur mainly at the entrance and along the channel, respectively (*see* Renkin & Curry, 1979; Eqs. A6–A9 and A11–A15).

1. Hindrance to diffusion through a cylinder is

$$S_d^c \cdot F^c = (1-\alpha)^2 \cdot (1 - 2.105\alpha + 2.0865\alpha^3 - 1.7068\alpha^5 + 0.726\alpha^6)/(1 - 0.75857\alpha^5). \quad (1)$$

2. Hindrance to diffusion through a slit is

$$S_d^s \cdot F^s = (1-\lambda) \cdot (1 - 1.004\lambda + 0.418\lambda^3 - 0.210\lambda^4 - 0.169\lambda^5). \quad (2)$$

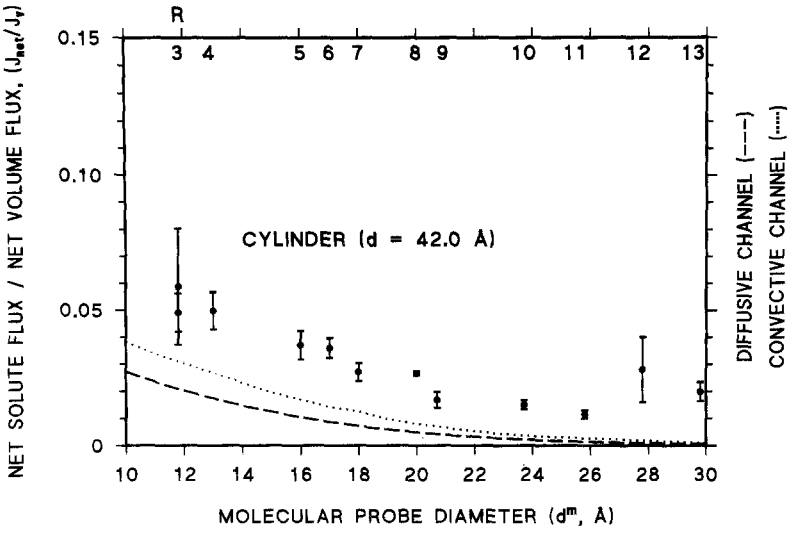

Fig. 6. Plot of (J_{net}/J_v) for probes with d^m 11.8–30.0 Å as a function of d^m (as in Fig. 5). Neither the dashed nor the dotted lines (diffusive and convective flows through a cylinder with d = 42.0 Å for 0.089 of the flow area, calculated using Eqs. 1, 3 and 5*a*) fit the data.

3. Hindrance to convection through a cylinder is

$$S_f^c \cdot G^c = [2(1-\alpha)^2 - (1-\alpha)^4] \cdot (1 - 0.667\alpha^2 - 0.20217\alpha^5)/(1 - 0.75857\alpha^5). \quad (3)$$

4. Hindrance to convection through a slit is

$$S_f^s \cdot G^s = (1 - 1.5\lambda^2 + 0.5\lambda^3) \cdot (1 - 0.333\lambda^2). \quad (4)$$

Flow Equations

With Eqs. 1–4 we can now write Eqs. 5 which describe restricted nonelectrolyte movement by diffusion and convection in a channel (*see* Steward, 1982, Eq. A2)

$$j(x)/A = -S_d \cdot F \cdot D \cdot (dC/dx)(x) + S_f \cdot G \cdot v(x) \cdot C(x) \quad (5)$$

which is integrated for cylinders as Eq. 5a and for slits as Eq. 5b

$$J_{net}{}^c = S_f^c \cdot G^c \cdot \beta \cdot J_v \, [C_c \cdot \exp(\phi^c) - C_t]/[\exp(\phi^c) - 1] \quad (5a)$$

where $\phi^c = (S_f^c \cdot G^c \cdot \beta \cdot J_v \cdot 4X/S_d^c \cdot F^c \cdot N \cdot \pi d^2 \cdot D)$;

$$J_{net}{}^s = S_f^s \cdot G^s \cdot \beta \cdot J_v \, [C_c \cdot \exp(\phi^s) - C_t]/[\exp(\phi^s) - 1] \quad (5b)$$

where $\phi^s = (S_f^s \cdot G^s \cdot \beta \cdot J_v \cdot X/S_d^s \cdot F^s \cdot w \cdot L \cdot D)$.[1]

[1] Parenthetically, if ϕ^c and ϕ^s have small values, Eqs. 5a and 5b approximate (Steward, 1982) to Eq. 6, the Kedem & Katchalsky (1958) equation

$$J_{net} = P \cdot \Delta C + (1 - \sigma) \cdot \beta \cdot J_v \cdot C^* \quad (6)$$

For cylinders, Eq. 6a takes the form of Eqs. 6a and 6a1

Morphology

The Lateral Intercellular Space (LIS) dimensions used are (Table 4; Fig. 7). L = 280–385 cm/cm^2 of epithelium (Whittembury, 1967); w = 164 μm. Area in the same plane, 3.77–6.31 10^{-4}cm/cm^2; X = 20 μm; septate junction depth, X_j = 7 μm; depth of the nonseptated part of LIS, X_{LIS} = 13 μm.

Fit of Models to the Experimental Results

Eqs. 5 were used to fit (following the approach of Hill & Shachar-Hill, 1993 and Shachar-Hill & Hill, 1993) the experimental data of Fig. 2 with diffusion and convection models of restricted flow through cylinders (Eqs. 5*b*, 1 and 3) and slits (Eqs. 5b, 2 and 4) of various diameters and widths, respectively. The results are shown in Figs. 3 to 6. As probes with $d^m > 30.0$ Å do not cross the tubule wall, 30.0 Å was taken, as a first approximation, as an upper limit to channel width. It may be seen in Fig. 3, that for a 30 Å-wide slit the diffusive flow model fits only the first 3 and the last 4 of the 19 probes explored. It does not fit the 12 probes of intermediate d^m. The

$$J_{net}{}^c = P^c \cdot \Delta C + (1 - \sigma^c) \cdot \beta \cdot J_v \cdot C^* \quad (6a)$$

$$J_{net}{}^c = (S_d^c \cdot F^c \cdot N \cdot \pi d^2 \cdot D/4X) \cdot \Delta C + S_f^c \cdot G^c \cdot \beta \cdot J_v \cdot C^* \quad (6a1)$$

where $P^c = S_d^c \cdot F^c \cdot N \cdot \pi d^2 \cdot D/4X$, and $(1 - \sigma^c) = S_f^c \cdot G^c$. For slits, it takes the form of Eqs. 6*d* and 6*e*

$$J_{net}{}^s = P^s \cdot \Delta C + (1 - \sigma^s) \cdot \beta \cdot J_v \cdot C^* \quad (6b)$$

$$J_{net}{}^s = (S_d^s \cdot F^s \cdot w \cdot L \cdot D/X) \cdot \Delta C + S_f^s \cdot G^s \cdot \beta \cdot J_v \cdot C^* \quad (6b1)$$

where $P^s = S_d^s \cdot F^s \cdot w \cdot L \cdot D/X$, and $(1 - \sigma^s) = S_f^s \cdot G^s$.

Table 4. Some dimensions of the 5th instar UMT

Cell diameter (μm)	100	[a]
Cell height, X, (μm)	20 (16–22)	[a]
	15	[b]
Septate junction height, X_j, (μm)	7.5 (7–8)	[a]
width, w, (Å)	164 (±15)	[a]
	170	[b]
	178	[c]
LIS height, X_{LIS}, (μm)[d]	12–14	[a]
Junctional linear extension,	280–385	[a]
L, (cm/cm^{2e})	229.4	[b]
LIS fractional area, wL,	3.77–6.31	[a]
(10^{-4} cm^2/cm^2)	3.9	[b]

See Fig. 7. [a]Present work and Whittembury et al., 1986; calculated following Whittembury, 1967. [b]O'Donnell & Maddrell, 1983. [c]Lane & Skaer, 1980; Skaer, Harrison & Lee, 1979. [d]LIS height not occupied by the septate junction. [e]in a plane parallel to the epithelial surface per cm^2 of epithelium; no brush border or basolateral infoldings are taken into consideration.

convective flow model for a 30 Å-wide slit is worse. Cylinder models (*not shown*) are even worst fits.

It was not possible to fit all data with a single-sized channel. Therefore, models of two parallel channels were explored, one to fit 8 *group a* probes and another to fit *group b* probes.

Group A Probes

Convection through an 11.0 Å-wide slit is the best fit, while convection through a cylinder (d = 11.0 Å) is not (Fig. 4). A 12 Å-wide slit was previously proposed using a model that needed information about σ values. σ could not be measured directly. Therefore, σ values had to be estimated leading to some uncertainty in the slit width proposition (Whittembury et al., 1986). To circumvent this difficulty, in the present work, models are independent of σ values. Therefore the present modeling has a more solid founding. The 11.0 Å-wide slit is a much better fit than the previously proposed 12 Å-slit. A diffusion model through the septate junction (an 11.0 Å-wide, 7 μm-deep slit) accounts for only 0.0828 times the observed flow (Fig. 4, curve *d; Table 5*), because the resistance to diffusion along such a deep structure is very large. Wider slits also fail to fit (Fig. 3).

Group B Probes

As models of wide channels with flow through all the flow area did not fit the data for these probes (Fig. 3), models were tried with a smaller flow area. A diffusive flow model through a 42.0 Å-wide slit, with only 0.089 of the flow area, provided the best fit (Fig. 5). 0.089 is not statistically different from 0.0713 ± 0.0101, the linear regression intercept (Fig. 2). Convective models through slits or cylindrical channels did not fit the data (Fig. 6).

Table 5. Junctional flows

Probe	Diffusive flow 10^{-12} moles/cm^2 · sec	Flow ratio diffusive/convective
Water	0.7–1.3	0.04–0.068
Urea	0.3–0.4	0.02–0.021
Erythritol	0.1–0.16	0.005–0.008
Mannitol	0.03–0.06	0.0016–0.003
Sucrose	0.01–0.02	0.0005–0.001

Parameters calculated using Eqs. 5*b* and 6, the known probes diffusion coefficients and the morphological parameters given in Table 4 (*see text*). Figure 4 shows these data as J_{net}/J_v *vs.* d^m, best fitted by the equation $100 \cdot (J_{net}/J_v) = 8.28\ (\pm 2.13) - 1.01\ (\pm 0.29)\ J_v$; ($r = -0.89 \pm 0.27$; $P < 0.001$).

In short, two different approaches lead to conclude that *group a probes* are solvent-dragged. First, the observation that the slopes of plots of J_{net} *vs.* J_v (Table 2) are significantly larger than 0 in the absence of USL effects. Second, there is only one model that fits the first part of Fig. 2, namely convection through an 11.0 Å-wide slit. A second conclusion is that a diffusion model through a 42.0 Å-wide slit (in parallel with the 11.0 Å-wide slit) is required to fit data from *group b* probes (Fig. 5).

Pathways for Flow

Water could cross the epithelium through the cells using route A in Fig. 7. It would have to move first through one cell membrane, then dissolve in the cytosol to approach the other cell membrane to finally cross it. If this were the case it could not drag solutes, since it would move by diffusion in the cytosol (Ussing & Eskesen, 1989; Nielsen & Ussing, 1992, 1993). We have shown here that water drags all *group a* probes. The dragged solutes range in size from small (urea and erythritol) to "extracellular markers" (sucrose and dextrans *1, 2* and *3;* the latter has a d^m = 11.8 Å), which do not cross the cell membrane (Whittembury et al., 1986). Therefore, water must flow through a noncytosolic pathway that can be acceded by those extracellular markers. The pathway must be an 11.0 Å-wide slitlike structure. As the model is a convection (and not a diffusion model) that fits all *group a* probes including water as a single function it must be concluded that most water during secretion must follow this pathway. This conclusion is based (i) in that *group a* probes are solvent dragged. (ii) Plots of J_{net}/J_v *vs.* d^m for *group a* probes are best fitted with a model for convection through 11.0 Å-wide slits that occupy most of the flow area. Water, urea and erythritol enter the cell.

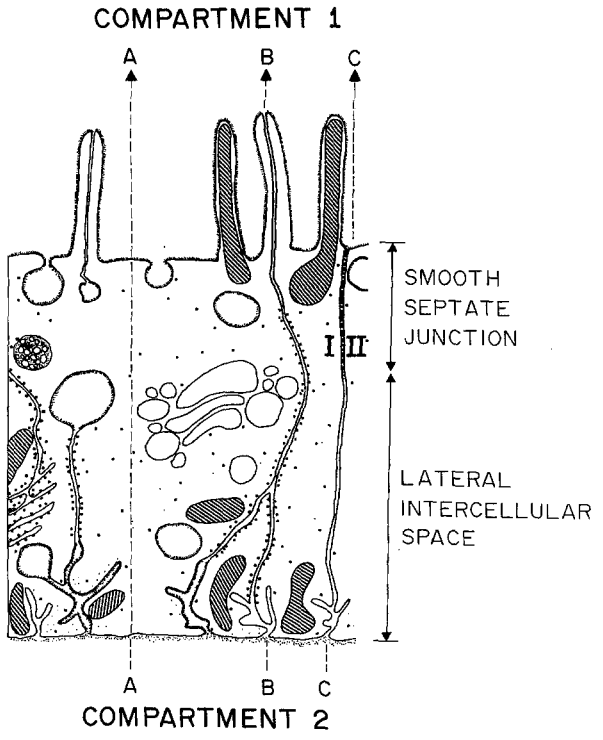

Fig. 7. UMT cells I and II with possible pathways for transepithelial water flow (schematic, not to scale). In the 5th instar their average diameter is 100 μm. Two cells complete one tubule circumference (Whittembury et al., 1986). (*See* Table 4). Using pathway *A*, water would cross one cell membrane, dissolve in the cytosol, diffuse towards the other cell membrane, and move through it. Pathway *B* follows the lateral intercellular space (LIS). The latter is formed by the quasi parallel lateral membranes of adjacent cells, separated by a distance of 164 Å. It has a depth *X* of some 20 μm. About one third of its luminal end shows 7 to 8 μm-deep smooth septate junctions which contact the tubule lumen (compartment 1) at their apical end. The junctions continue at 0.5 μm-thick basement membrane and the haemolymph (compartment 2). LIS extends linearly, in a plane parallel to the lumen surface, for 230–385 cm/cm^2 of tubule area. Pathway *C* schematizes sets of several μm-long parallel lines that cross the cell from basal end to the tip of some microvilli. They must represent sections of slit-forming membranes separated by a distance of 112 Å.

However, the observation that there is a monotonic relation between J_{net}/J_v and d^m for *group a* probes indicates that water, urea and erythritol must also flow across the epithelium via 11.0 Å-wide slits to be solvent dragged. *Group b* probes must diffuse through 42.0 Å-wide slits that occupy 0.089 of the flow area. Where are the transepithelial routes for these two groups of probes? In Fig. 7, one possible route is pathway B (an endoplasmic reticulum 112 Å-wide pathway which extends from basal cell membrane to the tip of some microvilli; Whittembury et al., 1986; Berthelet et al., 1987). Pathway B must be shaped as a slit, since the sets of parallel lines in the electronmicrographs that constitute this structure extend over lengths of several μm. The most obvious route is pathway C, formed by the 164 Å-wide septate junctions and LIS, which are permeated by Lanthanum (Lane & Skaer, 1980). Pathways B and C could be filled with materials that effectively narrow them. For example the 40–60Å septa (in the septate junctions, Skaer et al., 1979; Lane & Skaer, 1980) could also be filled by some other material. The spaces in a uniform suspension of fibers may behave as a porous material (Ogston, 1958). Secretion would flow through the 11.0 Å-wide, most abundant pathway, dragging *group a* probes and diffusion for *group b* probes through another route. It has been pointed out that the site of any (possible) osmotic equilibration would be the luminal microvilli (McElwain, 1984) but solutes leaving or entering the junctions only traverse a minute area fraction of this system, which cannot contribute to the observed drag. As illustrated in Fig. 4, diffusion explains only a small fraction of the observed J_{net}/J_v flow ratio for *group a* probes. The 42.0 Å-wide, less abundant pathway must be separate from the first one. But at present we do not know enough to choose between these possibilities.

E.G. is a Visiting Scientist at IVIC. It is a pleasure to thank Drs. A.E. Hill and Bruria Shachar-Hill for their suggestion of the use of dextrans, their instruction and help with the dextran separation technique, and their extensive discussions. Dr. R. Apitz, Mr H. Rojas and Mrs. Fulvia Bartoli were most helpful with suggestions during the course of the experimental work. Mr. Jose Mora was fundamental help with the equipment. Mrs. Lelis Ochoa and Mr. Luis F. Alvarez helped with some of the drawings. This work was partially supported by CONICIT, Fundación Polar and CDCH of UCV. It is a pleasure to thank Dr. H. Passow and Dr. K.J. Ullrich at the Max Planck Institut für Biophysik (Frankfurt/Main) where this work was initiated.

References

Barry, P.H., Diamond, J.M. 1984. Effects of unstirred layers on membrane phenomena. *Physiol. Rev.* **64:**736–872

Bean, C.P. 1972. The physics of porous membranes. *In:* Membranes, G. Eisenman, editor. Vol. 1, pp. 1–54. Marcel Dekker, New York

Berthelet, F., Beaudry-Lonergan, M., Linares, H., Whittembury, G., Bergeron, M. 1987. Polimorphic organization of the endoplasmic reticulum of the Malpighian tubule. Evidence for a transcellular route. *La Cellule.* **74:**281–293

Carpi-Medina, P., Lindemann, B., González, E., Whittembury, G. 1984. The continuous measurement of tubular volume changes in response to step changes in contraluminal osmolality. *Pfluegers Arch.* **400:**343–348

Deetjen, P. 1978. Microperfusion of superficial tubules and peritubular capillaries. *In:* Andreucci, V.E., Manual of Renal Micropuncture. pp. 208–218. Idelson, Naples

Hill, A.E., Shachar-Hill, B. 1993. A mechanism for isotonic fluid flow through the tight junctions of *Necturus* gallbladder epithelium. *J. Membrane Biol.* **136:**253–262

Kedem, O., Katchalsky, A. 1958. Thermodynamics analysis of the permeability of biological membranes to nonelectrolytes. *Biochim. Biophys. Acta.* **27:**229–246

Kristensen, P., Ussing, H.H. 1992. Epithelial Organization. *In:* The Kidney, Physiology and Pathophysiology, D.W. Seldin and G. Giebisch, editors. pp. 265–286. Raven Press, New York

Lane, N.J., Skaer, H. leB. 1980. Intercellular junctions in insect tissues. *Adv. Insect Physiol.* **15:**35–213

Maddrell, S.H.P. 1980. Characteristics of Epithelial transport in Mal-

pighian Tubules. *Curr. Topics in Membranes & Transport.* **14:**427–463

Maddrell, S.H.P., Herman, W.S., Farndale, R.W., Riegel, J.A. 1993. Synergism of hormones controlling epithelial fluid transport in an insect. *J. Exp. Biol.* **174:**65–80

Maddrell, S.H.P., Herman, W.S., Mooney, R.L., Overton J.A. 1991. 5-Hydroxytryptamine: a second diuretic hormone in *Rhodnius prolixus. J. Exp. Biol.* **156:**557–566

McElwain, D.L.S. 1984. A theoretical investigation of fluid transport in the Malpighian tubules of an insect, *Rhodnius prolixus* Stål. *Proc. R. Soc. London B.* **222:**363–372

O'Donnell, M.J., Aldis, S.K., Maddrell, S.H.P. 1982. Measurements of osmotic permeability in the Malpighian tubules of an insect, *Rhodnius prolixus* Stål. *Proc. R. Soc. London B.* **216:**267–277

O'Donnell, M.J., Maddrell, S.H.P. 1983. Paracellular and transcellular routes for water and solute movements across insect epithelia. *J. Exp. Biol.* **106:**231–253

O'Donnell, M.J., Maddrell, S.H.P., Gardiner, B.O.C. 1984. Passage of solutes through walls of Malpighian tubules of *Rhodnius* by paracellular and transcellular routes. *Am. J. Physiol.* **246:**R759–R769

Ogston, A.G. 1958. The spaces in a uniform suspension of fibres. *Trans. Faraday Soc.* **54:**1754–1757

Renkin, E.M., Curry, F.E. 1979. Transport of water and solutes across capillary endothelium. *In:* Membrane Transport in Biology. Vol IV-A. G. Giebisch, DC Tosteson and H.H. Ussing, editors. pp. 1–45. Springer Verlag, New York

Shachar-Hill, B., Hill, A.E. 1993. Convective fluid flow through the paracellular system of *Necturus* gallbladder epithelium as revealed by dextran probes. *J. Physiol.* **468:**463–486

Shipp, J.C. Hanenson, I.B., Windhager, E.E., Schatzmann, H.J., Whittembury, G., Yoshimura, H., Solomon, A.K. 1958. Single proximal tubules of the *Necturus* Kidney. Methods for micropuncture and microperfusion. *Am. J. Physiol.* **195:**563–569

Skaer H. leB., Harrison, J.B., Lee, W.M. 1979. Topographical variation in the structure of the smooth septate junction. *J. Cell Sci.* **37:**373–389

Steward, M.C. 1982. Paracellular nonelectrolyte permeation during fluid transport across rabbit gallbladder epithelium. *J. Physiol.* **322:**419–439

Ussing, H.H., Eskesen, K. 1989. Mechanism of isotonic water transport in glands. *Acta Physiol. Scand.* **136:**443–454

Wessing, A. 1965. Die Funktion der Malpigischen Gefaesse. *In:* Funktionelle und Morphologische Organisation der Zelle: Sekretion und Exkretion. K.E. Wohlfarth-Bottermann, editor. pp. 228–268. Springer Verlag, Berlin

Whittembury, G. 1967. Sobre los mecanismos de absorción en el túbulo proximal del riñón. *Acta Client. Venezol.* **18:**(Suppl. 3)43–56

Whittembury, G., Reuss, L. 1992. Mechanisms of coupling of solute and solvent transport in epithelia. *In:* The Kidney, Physiology and Pathophysiology, D.W. Seldin and G. Giebisch, editors. pp. 317–360. Raven Press, New York

Whittembury, G., Biondi, A.C., Paz-Aliaga, A., Linares, H., Parthe, V., Linares, N. 1986. Transcellular and paracellular flow of water during secretion in the upper segment of the Malpighian tubule of *Rhodnius prolixus:* solvent drag of molecules of graded size. *J. Exp. Biol.* **123:**71–92